

Synthesis of Titanium Diboride Layers under the High-Power Electron Beam in Vacuum

N.K. Galchenko, K.A. Kolesnikova, and O.K. Lepakova*

Institute of Strength Physics and Materials Science SB RAS, 2/1, Akademicheskoy ave., Tomsk, 634021, Russia

Fax: +8(3822) 28-69-66, Email: Kolesnikova_KsAl@mail.ru

**Department of structural Macrokinetics of the Tomsk Scientific Centre of the SB RAS,
10/3, Akademicheskoy, Tomsk, 634021, Russia*

Abstract – The paper presents the investigation results for the structure and properties of composite coatings obtained from a mixture of thermoreactive FeB and FeTi powders by electron beam surfacing. The dependence of the coating phase and structure formation on the granulometric composition of initial components of the fused mixture is shown. The abrasive wear resistance, friction coefficients and wear rate in friction pairs are studied. The relation of the obtained characteristics to the structure and morphological features of the coating structural components is demonstrated.

1. Introduction

The wear resistant composite coatings on the basis of titanium borides, which are synthesized from thermoreactive powder components of a boron-containing mixture at electron beam surfacing, are interesting for applications today.

It is known that in electron beam surfacing of thermoreactive powders an additional amount of heat is released in the fusion zone due to the exothermal reaction between the mixture components. This allows, with the same electron beam power, the deposition of coatings with a required content of the fine-grained refractory component. The physico-mechanical properties of the coatings can vary in a wide range depending on the proportion and sizes of initial components in the fused mixture. The coating structure formation ends with the convective mixing of solid-liquid melts, which have formed after the complete dissolution of components having different viscosity because of different chemical composition and different content of refractory particles in them [1]. The degree of the melt mixing depends on many factors, including the size of initial components. Obviously, changes in the granulometric composition of the fused powder would greatly affect the crystallization rate, completeness of phase transformations at electron beam surfacing, thus defining the microstructure, phase composition, and service properties of deposited coating.

The aim of the paper is to study the simultaneous synthesis of boride compounds and formation of composite coatings on their basis under vacuum electron-beam treatment of thermoreactive powders.

2. Materials and experimental procedure

The mixture for the electron beam surfacing of coatings and their further examination was prepared of low-cost thermoreactive ferroalloy powders FeB (grade FB-20) and FeTi (grade FTi65) widely used in steel and alloy metallurgy.

Table 1. Chemical composition of ferroalloys (wt %) used in the study

Grade	B	Si	Al	C	S	P	Cu	Ti	V
FB-20	20	2	3	0,05	0,01	0.02	0.05	–	–
FTi65	–	1	5	0.4	0.05	0.05	0.4	65	3

The composite material with a definite proportion of the refractory compound (titanium diboride) and metal binder (iron) was produced by the chemical reaction $x\text{FeB} + y\text{FeTi} \rightarrow \text{TiB}_2 + \text{Fe} + Q$.

The mixture composition was calculated so that to produce the TiB₂-Fe composite coating with 33 mass % of titanium diboride. The given percentage is provided by the proportion of the used mixture components FeB-FeTi = 1:1.

To study the features of the phase and structure formation in the fused layer, three variants of FeB-FeTi powder mixtures were electron-beam deposited in experiments. The mixtures differed in the granulometric composition of initial components:

- 1) FeB(50–125 μm) + FeTi(200–315 μm);
- 2) FeB(200–315 μm) + FeTi(200–315 μm);
- 3) FeB(200–315 μm) + FeTi(50–200 μm).

The coatings were electron-beam deposited on steel substrates (grade St.3) in 2–4 passes at accelerating voltage 28 kV. The beam diameter was 1.0 mm, scanning length 12 mm, and substrate velocity 2 mm/s. The fused layer thickness was 2–3 mm.

The phase composition was X-ray examined by a diffractometer DRON-4, the chemical composition was studied by a setup KAMEBAX-MIKROBEAM for X-ray spectrum microanalysis on an area of 1 μm. The coating microstructure was examined by a light microscope MIM-9. The hardness H of the main structural components was measured by nanoindentation using a CSEM Nano Hardness Tester under load 5 g. The microhardness H_μ was measured by a device PMT-3 under the load $P = 50$ g.

The tribological properties of the coatings were studied in friction pairs consisting of a stationary pin of hard alloy VK-6 and rotating disc. The pin hardness was $H_{\mu} = 29.3$ GPa. The tests were performed at room temperature with and without lubrication (N20 + SMT) of the contact zone by a PC-controlled high temperature tribometer THT-S-AX0000 under load 10 N and sliding velocities $V = 5$ and 11 cm/s. The major wear parameters of coatings in the friction pair were determined by the stabilization of the friction coefficient and linear wear in the course of continuous sliding after running-in.

3. Experimental results and discussion

3.1. Coatings of thermoactive powder mixture

FeB(50–125 μm) + FeTi(200–315 μm) (coating 1)

The comparative analysis has shown that the given coating has the most heterogeneous structure across the thickness. Fragments of the structure are depicted in Fig. 1. The structure is typically observed after the crystallization of melts of nonuniform concentration. The uneven microhardness distribution across the coating thickness clearly demonstrates its heterogeneity (Fig. 4, *a*).

The performed investigation suggests the following mechanism of structure formation at surfacing. First, FeTi particles of size 200–315 μm melt ($T_m = 1200$ °C) and form a ferrotitanium melt. When contacting with a conglomerate of FeB particles ($T_m = 1540$ °C), the melt forms a ring structure around the FeB particles due to the formation of low-temperature contact eutectics. The ring structure consists of titanium diboride crystals of hardness $H = 38$ GPa (Fig. 1, *b*). The formation of the liquid phase – ferrotitanium melt – favors further refinement of the FeB particles that rapidly dissolve in the FeTi melt and saturate it with boron. The final coating structure is a result of the solidification of the two heterogeneous melts.

Since the electron beam surfacing is carried out in many passes, the deposition of next layers increases the substrate temperature, lifetime of the liquid metal bath formed on the surface of the underlying deposited layer and reduces the melt crystallization rate. After the crystallization the matrix structure of the composite coating is an alloyed solid solution with highly nonuniform concentration, fine and coarse iron and

titanium borides as well as with numerous nonequilibrium boride-based eutectics. This structure leads to the formation of heterogeneous coatings.

Figure 1, *c* illustrates the microstructure of the FeB(50–125 μm) + FeTi(200–315 μm) coating surface with solitary titanium diboride crystals, which evidently entered the melt due to convective mass transfer from the underlying layer in the middle of the coating. There is a structure on the coating surface which consists of large titanium diboride crystals (7–22 μm) and heterogeneous metal binder with non-uniform hardness. The binder is chaotically hardened by fine-grained (≤ 1 μm) compounds of titanium borides of other stoichiometry (Fig. 1, *c*). This is confirmed by the data of X-ray phase analysis showing that, along with pronounced reflections from TiB_2 and $\alpha\text{-Fe}$, phases TiB , Ti_2B , and Ti_2B_5 are registered.

3.2. Coatings of thermoreactive powder mixture

FeB(200–315 μm) + FeTi(200–315 μm) (coating 2)

The microstructural analysis of coatings produced of a mixture of coarse-grained powders having the same granulometric composition (coating 2) has also shown that the coating structure is heterogeneous across the thickness (Fig. 2).

This is probably due to the fact that, because of the large powder particles and high crystallization rate, the time period when the concentration of alloying elements in the formed melt becomes uniform was too short. The nonuniform melt crystallization resulted in the formation of specific structures at the interface with the substrate and in the middle of the deposited layer. The structures have irregularly shaped regions in the form of light unetched globules whose chemical composition differs across the coating thickness. By the data of X-ray spectrum microanalysis, the above solid solution regions at the interface have the composition of Fe_2B and hardness $H \approx 14$ GPa (Fig. 2, *a*). In the middle of the coating (Fig. 2, *c*) the globules became three-dimensional and darker in color. These regions have the composition of FeB and hardness $H = 16$ –18 GPa. The FeB formation is evidently caused by the fact that with distance from the coating – substrate interface and increasing number of passes the melt temperature grows and the degree of its saturation with boron also increases owing to a more complete dissolution of initial FeB powder particles.

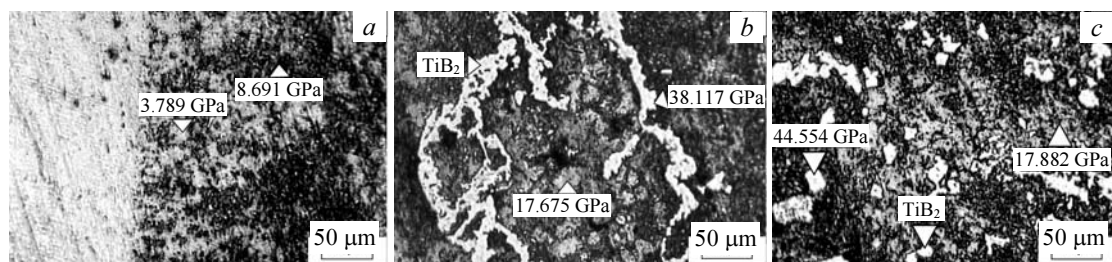


Fig. 1. Microstructure of the coating produced of thermoreactive powder mixture FeB(50–125 μm) + FeTi(200–315 μm): *a* – interface with the substrate; *b* – middle of the deposited layer; *c* – subsurface coating area

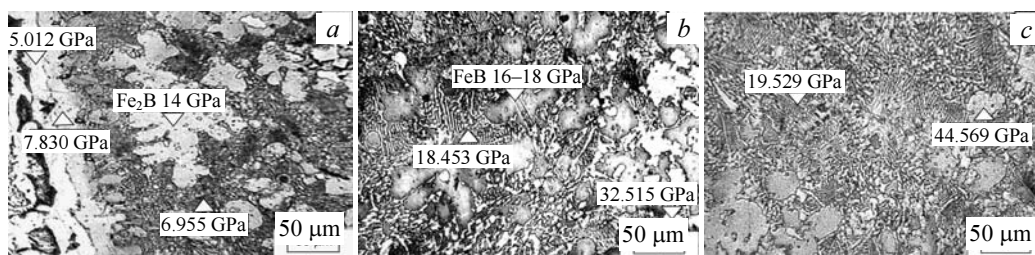


Fig. 2. Microstructure of the coating produced of thermoreactive powder mixture FeB(200–315 μm) + FeTi(200–315 μm): a – interface with the substrate; b – middle of the deposited layer; c – subsurface coating zone

Such melt crystallizes with the formation of regions in the coating structure which have the composition of FeB, being separated by fine-grained particles and their conglomerates whose hardness ($H = 32.5$ GPa) corresponds to the TiB₂ phase. One can also see from Figs. 2, b and c that the metal binder structure between the unetched regions exhibits heterogeneous phase morphology and nonuniform hardness ($H = 6–19$ GPa). It has numerous regions with dendritic and eutectic structure whose hardness reduces with the eutectic size refinement. According to the X-ray phase analysis, the eutectics can be the Fe₂B–Fe and TiB₂–Fe compounds [2, 3].

When surfacing powders of the given granulometric composition, we observed the highest fluidity of the formed melt as compared to coatings 1 and 3.

3.3. Coatings of thermoreactive powder mixture FeB(200–315 μm) + FeTi(50–200 μm) (coating 3)

After coating deposition, we had a layered structure, in which every layer mainly contained one phase component across its thickness (Fig. 3).

In the middle of the coating at 1.3 mm from the interface with the substrate (Fig. 3, b) the structure mainly consists of rounded Fe₂B particles of size 8–12 μm and hardness $H = 14.4$ GPa, rectangular titanium diboride crystals (4–6 μm) and larger elongated titanium boride particles embedded in the Fe₂B–Fe eutectic matrix. The subsurface coating region (Fig. 3, c) also has heterogeneous phase composition: the left part of the microscan demonstrates aggregates of titanium borides, the right part – a microstructure region with uniform distribution of 10–17 μm light crystals in the metal binder which are titanium borides and diborides (TiB, TiB₂). The hardness of the particles is in the interval $H = 22–34$ GPa.

To find whether titanium borides can be used as the solid phase, we studied its abrasive and structural wear resistance in dry sliding friction and lubricated friction. The wear resistance in both abrasive and friction wear is found to correlate with the aggregate hardness of the deposited Fe–B–Ti coatings and depend on the volume fraction of the refractory component in the surface region, phase morphology and degree of metal binder hardening (Table 2).

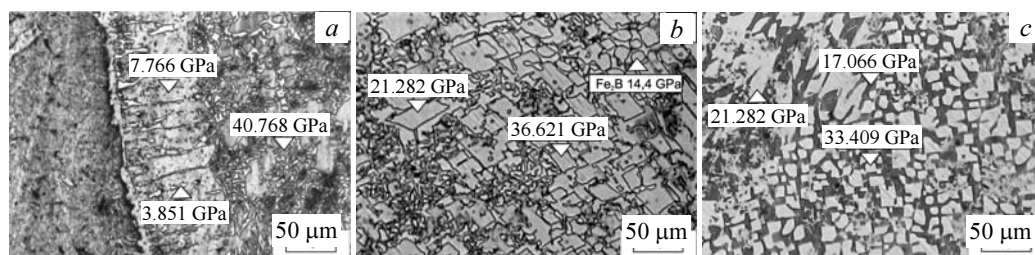


Fig. 3. Microstructure of the coating produced of thermoreactive powder mixture FeB(200–315 μm) + FeTi(50–200 μm): a – interface with the substrate; b – middle of the deposited layer; c – subsurface coating region

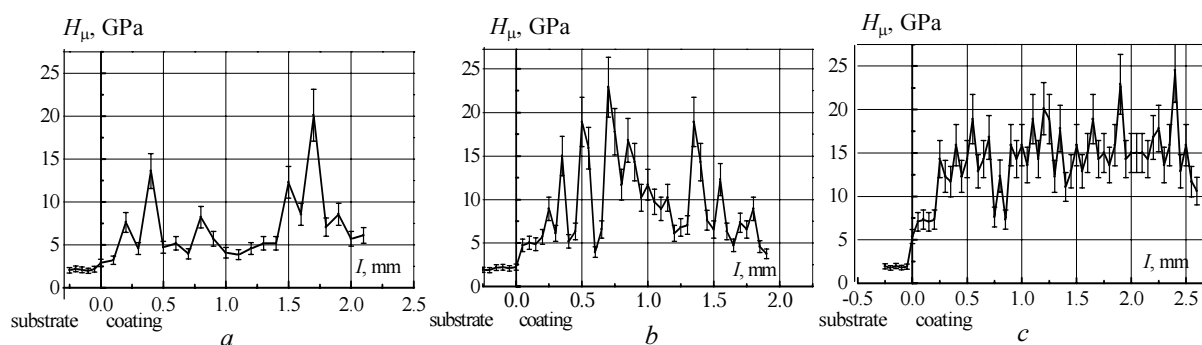


Fig. 4. Distribution of microhardness H_{μ} in the coating: a – FeB(50–125 μm) + FeTi(200–315 μm); b – FeB(200–315 μm) + FeTi(200–315 μm); c – FeB(200–315 μm) + FeTi(50–200 μm)

Table 2. Friction coefficient f , wear rate I ($\mu\text{m}/\text{km}$), wear coefficient K_w , and microhardness (GPa) of coatings produced by electron beam surfacing

Coating composition	Friction coefficient, f_{wear}		Wear rate, I , $\mu\text{m}/\text{km}$		Coating surface hardness, GPa	K_w
	5 cm/s	11 cm/s	5 cm/s	11 cm/s		
FeB(50–125) + FeTi(200–315)	min – 0.142 max – 0.702 aver. – 0.433	min – 0.16 max – 0.618 aver. – 0.31	2.28	1.29	5–7	1.86
FeB(200–315) + FeTi(200–315)	min – 0.148 max – 0.803 aver. – 0.526	min – 0.160 max – 0.633 aver. – 0.395	2.32	1.45	10–12	5.72
FeB(200–315) + FeTi(50–200)	min – 0.153 max – 0.632 aver. – 0.515	min – 0.168 max – 0.594 aver. – 0.517	1.61	3.31	15–20	11.3

The comparative analysis of the microstructures and abrasive wear resistance has shown that the most favorable structures in the given wear mode are obtained from the powder mixtures FeB(200–315 μm) + FeTi(200–315 μm) (coating 2) and FeB(200–315 μm) + FeTi(50–200 μm) (coating 3). The high wear resistance of coating 2 ($K_w = 5.72$) is evidently due to the regular structure and very fine grain size of eutectic components of the metal binder. Coatings 3, where the major phases are titanium borides, have the highest aggregate hardness and abrasive wear resistance ($K_w = 11.3$). Coatings 1 exhibit the maximum wear rate. They have the most heterogeneous structure with low metal binder microhardness ($H_\mu = 4\text{--}5$ GPa), in which X-ray spectrum microanalysis revealed numerous regions of iron free from fine-grained particles. During wear the abrasive material acted mainly upon the ductile matrix, thus governing its high wear rate and spalling of titanium boride crystals.

The dry friction test in a friction pair with a hard alloy pin has shown that the wear rate of the deposited coatings is within 1.29–3.31 $\mu\text{m}/\text{km}$. The sliding velocity growth reduces the friction coefficient and wear rate in coatings 1 and 2. This is probably caused by the temperature elevation in the contact patch and formation of secondary structures on friction surfaces because of tribooxidation.

The friction coefficients at the chosen sliding velocities ($V = 5.11$ cm/s) are in the intervals 0.43–0.52 and 0.31–0.39, respectively. In contrast to the first two compositions, for coating 3, whose surface layer has a high concentration of titanium boride particles synthesized in surfacing and low binder content, the sliding velocity growth did not change the friction coefficient. However, owing to the reducing ductility of the sub-

surface layer and cracking of solid particles, the sliding velocity growth increased two times the coating wear rate in the given range of sliding velocities: from 1.61 to 3.3 $\mu\text{m}/\text{km}$. The lubricant application in the friction zone greatly enhanced the tribological properties of all the coatings.

4. Conclusions

1. The electron beam surfacing of thermoreactive Fe–B–Ti powders allows producing composite coatings on the basis of refractory titanium borides synthesized under the electron beam in vacuum. Such coatings exhibit high abrasive wear resistance and low wear rate in dry friction.

2. The granulometric composition of the fused powder mixtures strongly influences the physico-chemical processes occurring in the molten bath under the electron beam. It defines the coating properties that depend on the structure, proportion of boride phases and the metal binder, and the degree of solid solution hardening.

3. The composite coatings produced of Fe–B–Ti system by electron beam surfacing can be applied as wear resistant materials.

References

- [1] N.K. Galchenko, S.I. Belyuk, V.E. Panin et al., *Fiz. Khim. Obrab. Mater.* **68/4** (2002).
- [2] V.E. Panin, S.I. Belyuk, V.G. Durakov, G.A. Pribytkov, and N.G. Rempe, *Svarochnoe Proizvodstvo* **34/2** (2000).
- [3] V.E. Panin, S.I. Belyuk, V.G. Durakov et al., *Electron Beam Surfacing Method, RF Patent 2205094 of May 27, 2003.*